Progress In Electromagnetics Research, PIER 86, 19–37, 2008

NOVEL BLIND JOINT DIRECTION OF ARRIVAL AND POLARIZATION ESTIMATION FOR POLARIZATION-SENSITIVE UNIFORM CIRCULAR ARRAY

X. Zhang, Y. Shi, and D. Xu

Electronic Engineering Department
Nanjing University of Aeronautics & Astronautics
Nanjing 210016, China

Abstract—A novel blind Direction of arrival (DOA) and polarization estimation method for polarization-sensitive uniform circular array is investigated in this paper. An analysis of the received signal of the polarization-sensitive uniform circular array shows that the received signal has trilinear model characteristics, and hence trilinear decomposition-based blind DOA and polarization estimation for polarization sensitive uniform circular array is proposed in this paper. Our proposed algorithm has better DOA and polarization estimation performance. Our proposed algorithm can be thought of as a generalization of ESPRIT, and has wider application than ESPRIT method. The useful behavior of the proposed algorithm is verified by simulations.

1. INTRODUCTION

Polarization is an important characteristic of the electromagnetic wave [1–7]. Polarization sensitive antenna arrays have some inherent advantages over traditional arrays, because they can separate signals based on their polarization characteristics. Intuitively, polarization sensitive antenna arrays will provide improved signal detection performance for signals having different polarization characteristics. Polarization sensitive arrays are used widely in the communication, radio and navigation [8–12]. Direction-of-arrival (DOA) estimation [13–17] is key technique in array signal processing or polarization sensitive array. The problems of estimating jointly direction-of-arrival (DOA) and polarization parameters of diversely polarized multiple cochannel signals have been considered in various

works [18–29]. There are many joint DOA and polarization estimation methods, including ESPRIT [19–22], MUSIC [23], Root-MUSIC [24], cumulants [25], cyclostationarity [26] and others [27–29]. In all of these methods, the ESPRIT algorithm exploits the invariance properties of polarization sensitive arrays, including uniform linear array and square array, so that both angle and polarization estimates may be computed. In [19], ESPRIT is used to estimate both the arrival directions and the polarizations of incoming plane waves with a uniform linear array of crossed dipoles. In [21], ESPRIT algorithm is used with a square array of crossed dipoles to estimate both the two-dimensional arrival angles and the polarization of incoming narrowband signals. ESPRIT is a closed-form eigen structure-based parameter estimation technique that requires the data to possess certain "invariance" structures. The direction matrix of uniform circular array does not have Vandermonde characteristics, rotational invariance model can not be constructed, and then ESPRIT algorithm fails to work. ESPRIT ideas have revolutionized sensor array signal processing. Interestingly, a general principle underlying ESPRIT has flourished independently in other scientific fields and disciplines, where it is commonly referred to in a variety of ways, including trilinear model or trilinear decomposition. Trilinear decomposition-based DOA and polarization estimation for polarization sensitive uniform circular array is investigated in this paper.

It is well known that most of signal processing methods are based on the theory of matrix, or the bilinear model. In general, matrix decomposition is not unique, since inserting a product of an arbitrary invertible matrix and its inverse in between two matrix factors preserves their product. Matrix decomposition can be unique only if one imposes additional problem-specific structural properties including orthogonality, Vandermonde, Toeplitz, constant modulus or finite-alphabet constraints. Compared with the case of matrices, trilinear model or trilinear decomposition has a distinctive and attractive feature: it is often unique [30]. The uniqueness of trilinear decomposition is of great practical significance, which is crucial in many applications such as psychometrics [31] and chemistry [32–34]. Trilinear decomposition is thus naturally related to linear algebra for multi-way data. In the signal processing field, trilinear decomposition can be thought of as a generalization of ESPRIT and joint approximate diagonalization ideas [35, 36]. Trilinear decomposition is used widely in blind receiver detection for Direct-sequence code-division multiple access system [37, 38], array signal processing [39, 40], blind estimation of Multi-Input-Multi-Output system [41] and blind speech separation [42].

Our work links the polarization-sensitive uniform circular array parameter estimation problem to the trilinear model and derives a novel blind DOA and polarization estimation. Our proposed algorithm has better DOA and polarization estimation performance. The algorithm does not require pilot information and train sequence. Instead, this method relies on a fundamental result of Kruskal [30] regarding the uniqueness of low-rank three-way data decomposition. ESPRIT method is a special case of our proposed algorithm. Our proposed algorithm is the generalization of ESPRIT. Our proposed algorithm has wider application than ESPRIT method.

This paper is structured as follows. Section 2 develops the data model. Section 3 deals with algorithmic issues and discusses identifiability issues. Section 4 presents simulation results. Section 5 summarizes our conclusions.

Denote: We denote by $(.)^*$ the complex conjugation, by $(.)^T$ the matrix transpose, and by $(.)^H$ the matrix conjugate transpose. The notation $(.)^+$ refers to the Moore-Penrose inverse (pseudo inverse). $\| \|_F$ stands for the matrix conjugate transpose. $\mathbf{I}$ is an identity matrix.

2. THE DATA MODEL

We consider an array with sensors at M different locations as shown in Fig. 1. The location geometry is circular with the radius R. Centered at each location, there are three orthogonal short dipoles, the x-, y-, and z-axis dipoles, parallel to the x, y, and z axes, respectively.

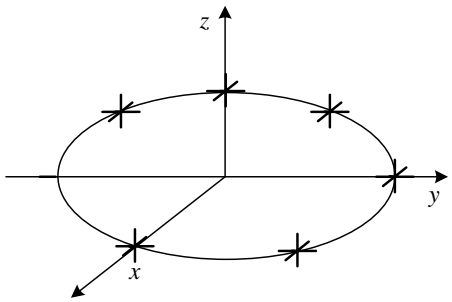

Figure 1. Structure of polarization sensitive uniform circular array.

2.1. The Signal Model for Polarization Sensitive Antenna

We begin by considering the polarization of an incoming signal. Suppose there is an antenna at the origin of a spherical coordinate

system. Assume that a signal $b(t)$ is arriving from direction θ, φ, where θ is the elevation angle and φ is the azimuth angle. Let this signal be a transverse electromagnetic (TEM) wave, and consider the polarization ellipse produced by the electric field in a fixed transverse plane. Polarization parameters are γ, η. We characterize the antenna in terms of its response to linearly polarized signals in the x, y and z directions. Let v_x be the complex voltage induced at the antenna output terminals by an incoming electromagnetic signal with a unit electric field polarized entirely in the x direction. Similarly, let v_y, v_z be the output voltages induced by signals with unit electric fields polarized in the y and z directions, respectively. The total output voltage from this antenna in response to the electromagnetic signal is

$$y_p(t) = \begin{bmatrix} v_x \\ v_y \\ v_z \end{bmatrix} = \begin{bmatrix} \cos\theta\cos\varphi & -\sin\varphi \\ \cos\theta\sin\varphi & \cos\varphi \\ -\sin\theta & 0 \end{bmatrix} \begin{bmatrix} \sin\gamma e^{j\eta} \\ \cos\gamma \end{bmatrix} b(t) = \mathbf{s}b(t) \quad (1)$$

where

$$\mathbf{s} = \begin{bmatrix} \cos\theta\cos\varphi & -\sin\varphi \\ \cos\theta\sin\varphi & \cos\varphi \\ -\sin\theta & 0 \end{bmatrix} \begin{bmatrix} \sin\gamma e^{j\eta} \\ \cos\gamma \end{bmatrix} \quad (2)$$

$\mathbf{s}$ is the polarization vector, and it relates to the polarization and DOA information.

2.2. The Signal Model for Polarization Sensitive Array

Assume that a signal $b(t)$ is arriving at the uniform circular array with M diversely polarized antennas. The received signal of the polarization sensitive uniform circular array is shown as follows.

$$y(t) = \left[q_0\mathbf{s}^{\mathrm{T}}, q_1\mathbf{s}^{\mathrm{T}}, \ldots, q_{M-1}\mathbf{s}^{\mathrm{T}}\right]^{\mathrm{T}} b(t) = (\mathbf{a} \otimes \mathbf{s})\, b(t) \quad (3)$$

where $\otimes$ stands for Kronecker product; $\mathbf{s}$ is the polarization vector, which is shown in (2). $q_m = \exp(j2\pi R\sin(\theta)\cos(\varphi - \phi_m)/\lambda)$. R is radius of circular array. $\phi_m = 2\pi m/M$. $\mathbf{a}$ is the short form of the direction vector $\mathbf{a}(\theta, \phi)$.

$$\mathbf{a}(\theta, \varphi) = \begin{bmatrix} \exp(j2\pi R\sin(\theta)\cos(\varphi - \phi_0)/\lambda) \\ \exp(j2\pi R\sin(\theta)\cos(\varphi - \phi_1)/\lambda) \\ \vdots \\ \exp(j2\pi R\sin(\theta)\cos(\varphi - \phi_{M-1})/\lambda) \end{bmatrix} \quad (4)$$

It is assumed that there are K sources impinging the polarization sensitive circular array, and the space time channel parameters are constant for L symbols. Define the source matrix $\mathbf{B} \in \mathbb{R}^{L\times K}$ as

$$\mathbf{B} = \begin{bmatrix} b_{1,1} & b_{2,1} & \cdots & b_{K,1} \\ b_{1,2} & b_{2,2} & \cdots & b_{K,2} \\ \vdots & \vdots & \ddots & \vdots \\ b_{1,L} & b_{2,L} & \cdots & b_{K,L} \end{bmatrix} \tag{5}$$

where $b_{k,l}$ is the lth symbol of the kth source.

When K sources impinge the polarization sensitive circular array, the received signal of the polarization sensitive array is given by

$$\mathbf{X} = [\mathbf{a}_1 \otimes \mathbf{s}_1, \mathbf{a}_2 \otimes \mathbf{s}_2, \ldots, \mathbf{a}_K \otimes \mathbf{s}_K]\, \mathbf{B}^T \tag{6}$$

where $\mathbf{a}_k$ and $\mathbf{s}_k$ are the array direction vector and polarization vector of the kth source, respectively.

Equation (6) can be denoted as

$$\mathbf{X} = [\mathbf{A} \circ \mathbf{S}]\mathbf{B}^T \tag{7}$$

where $\mathbf{A}\circ\mathbf{S}$ is Khatri–Rao product. $\mathbf{A}\cdot\mathbf{S} = [\mathbf{a}_1\otimes\mathbf{s}_1, \mathbf{a}_2\otimes\mathbf{s}_2 \ldots \mathbf{a}_K\otimes\mathbf{s}_K]$, where $\otimes$ stands for Kronecker product. $\mathbf{a}_k, \mathbf{s}_k$ are the k column of the matrix $\mathbf{A}$ and the matrix $\mathbf{S}$, respectively. $\mathbf{A} = [\mathbf{a}_1, \mathbf{a}_2, \ldots, \mathbf{a}_K] \in \mathbb{C}^{M\times K}$ is the direction matrix, $\mathbf{S} = [\mathbf{s}_1, \mathbf{s}_2, \ldots, \mathbf{s}_K] \in \mathbb{C}^{3\times K}$ is the polarization matrix. Eq. (7) can be denoted as

$$\mathbf{X} = \begin{bmatrix} \mathbf{X}_{..1} \\ \mathbf{X}_{..2} \\ \vdots \\ \mathbf{X}_{..M} \end{bmatrix} = \begin{bmatrix} \mathbf{S}D_1(\mathbf{A}) \\ \mathbf{S}D_2(\mathbf{A}) \\ \vdots \\ \mathbf{S}D_M(\mathbf{A}) \end{bmatrix} \mathbf{B}^T \tag{8}$$

where $D_m(.)$ is understood as an operator that extracts the mth row of its matrix argument and constructs a diagonal matrix out of it. $\mathbf{X}_{..m}$ can be denoted as

$$\mathbf{X}_{..m} = \mathbf{S}D_m(\mathbf{A})\mathbf{B}^T,\ m = 1, 2, \ldots, M \tag{9}$$

$\mathbf{X}_{..m}$ is regarded as the mth slice in spatial direction. For ESPRIT algorithm only uses two slices, like $\mathbf{X}_{..1} = \mathbf{S}\mathbf{B}^T$ and $\mathbf{X}_{..2} = \mathbf{S}\Phi\mathbf{B}^T$, where Φ is diagonal matrix.

In the presence of noise, the observation model becomes

$$\tilde{\mathbf{X}}_{..m} = \mathbf{X}_{..m} + \mathbf{V}_{..m} = \mathbf{S}D_m(\mathbf{A})\mathbf{B}^T + \mathbf{V}_{..m},\ m = 1, 2, \ldots, M \tag{10}$$

where $\mathbf{V}_{..m}$, the $3 \times \mathrm{L}$ matrix, is the received noise corresponding to the mth slice.

The signal in Eq. (9) is also denoted through rearrangements

$$x_{m,l,p} = \sum_{k=1}^{K} a_{m,k} b_{l,k} s_{p,k} \; m = 1, \ldots, M; \; l = 1, \ldots, L; \; p = 1, 2, 3 \tag{11}$$

where $a_{m,k}$ stands for the (m,k) element of $\mathbf{A}$ matrix, and similarly for the others. The signal in (11) is the trilinear model. The trilinear model reflects three kinds of diversity available: spatial, temporal and polarization diversity, as shown in Fig. 2.

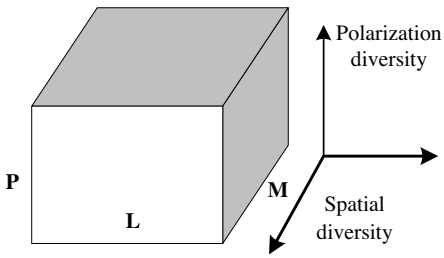

Figure 2. Trilinear model of the received signal.

3. BLIND DOA AND POLARIZATION ESTIMATION

3.1. Trilinear Decomposition

TALS (Trilinear Alternating Least Squares) algorithm is the common data detection method for trilinear model [30].

According to Eq. (8), the costing function of this trilinear model is

$$\min_{\mathbf{A},\mathbf{S},\mathbf{B}} \left\| \begin{bmatrix} \tilde{\mathbf{X}}_{..1} \\ \tilde{\mathbf{X}}_{..2} \\ \vdots \\ \tilde{\mathbf{X}}_{..M} \end{bmatrix} - \begin{bmatrix} \mathbf{S}D_1(\mathbf{A}) \\ \mathbf{S}D_2(\mathbf{A}) \\ \vdots \\ \mathbf{S}D_M(\mathbf{A}) \end{bmatrix} \mathbf{B}^T \right\|_F \tag{12}$$

where $\| \; \|_F$ stands for the Frobenius norm. $\tilde{\mathbf{X}}_{..m}, m = 1, 2, \ldots, M$, are the noisy slices. It follows that the least squares (LS) update for the

source matrix $\mathbf{B}$ is

$$\hat{\mathbf{B}}^T = \begin{bmatrix} \hat{\mathbf{S}}D_1\left(\hat{\mathbf{A}}\right) \\ \hat{\mathbf{S}}D_2\left(\hat{\mathbf{A}}\right) \\ \vdots \\ \hat{\mathbf{S}}D_M\left(\hat{\mathbf{A}}\right) \end{bmatrix}^+ \begin{bmatrix} \tilde{\mathbf{X}}_{..1} \\ \tilde{\mathbf{X}}_{..2} \\ \vdots \\ \tilde{\mathbf{X}}_{..M} \end{bmatrix} \tag{13}$$

where $[.]^+$ stands for pseudo-inverse. $\hat{\mathbf{A}}$ and $\hat{\mathbf{S}}$ denote previously obtained estimates of $\mathbf{A}$ and $\mathbf{S}$.

Equation (9) is regarded as slicing the three-way data along the spatial dimension. The symmetry of the trilinear model in Eq. (11) allows two more matrix system rearrangements,

$$\mathbf{Y}_{..p} = \mathbf{B}D_p(\mathbf{S})\mathbf{A}^T,\ p = 1, 2, 3 \tag{14}$$

$$\mathbf{Z}_{..l} = \mathbf{A}D_l(\mathbf{B})\mathbf{S}^T,\ l = 1, 2, \ldots, L \tag{15}$$

where $\mathbf{Y}_{..p}$ is the pth slice in polarization direction $\mathbf{Z}_{..l}$ is the lth slice in temporal direction. Similarly, from the second type of slices: $\mathbf{Y}_{..p} = \mathbf{B}D_p(\mathbf{S})\mathbf{A}^T$, $p = 1, 2, 3$, which is rewritten as

$$\begin{bmatrix} \mathbf{Y}_{..1} \\ \mathbf{Y}_{..2} \\ \mathbf{Y}_{..3} \end{bmatrix} = \begin{bmatrix} \mathbf{B}D_1(\mathbf{S}) \\ \mathbf{B}D_2(\mathbf{S}) \\ \mathbf{B}D_3(\mathbf{S}) \end{bmatrix} \mathbf{A}^T \tag{16}$$

According to symmetry of the trilinear model, the costing function in Eq. (14) is rewritten as follows

$$\min_{\mathbf{A},\mathbf{S},\mathbf{B}} \left\| \begin{bmatrix} \tilde{\mathbf{Y}}_{..1} \\ \tilde{\mathbf{Y}}_{..2} \\ \tilde{\mathbf{Y}}_{..3} \end{bmatrix} - \begin{bmatrix} \mathbf{B}D_1(\mathbf{S}) \\ \mathbf{B}D_2(\mathbf{S}) \\ \mathbf{B}D_3(\mathbf{S}) \end{bmatrix} \mathbf{A}^T \right\|_F \tag{17}$$

where $\tilde{\mathbf{Y}}_{..p}$, $p = 1, 2, 3$, are the noisy slices. $\hat{\mathbf{B}}$ and $\hat{\mathbf{S}}$ denote previously obtained estimates of $\mathbf{B}$ and $\mathbf{S}$. And the LS update for the direction matrix $\mathbf{A}$ is

$$\hat{\mathbf{A}}^T = \begin{bmatrix} \hat{\mathbf{B}}D_1\left(\hat{\mathbf{S}}\right) \\ \hat{\mathbf{B}}D_2\left(\hat{\mathbf{S}}\right) \\ \hat{\mathbf{B}}D_3\left(\hat{\mathbf{S}}\right) \end{bmatrix}^+ \begin{bmatrix} \tilde{\mathbf{Y}}_{..1} \\ \tilde{\mathbf{Y}}_{..2} \\ \tilde{\mathbf{Y}}_{..3} \end{bmatrix} \tag{18}$$

where $\hat{\mathbf{B}}$ and $\hat{\mathbf{S}}$ denote previously obtained estimates of $\mathbf{B}$ and $\mathbf{S}$.

Finally, from the third type of slices: $\mathbf{Z}_{..l} = \mathbf{A}D_l(\mathbf{B})\mathbf{S}^T$, $l = 1, 2, \ldots, L$. According to the symmetry of the trilinear model, the costing function in Eq. (14) is also rewritten as follows

$$\min_{\mathbf{A},\mathbf{S},\mathbf{B}} \left\| \begin{bmatrix} \tilde{\mathbf{Z}}_1 \\ \tilde{\mathbf{Z}}_2 \\ \vdots \\ \tilde{\mathbf{Z}}_L \end{bmatrix} - \begin{bmatrix} \mathbf{A}D_1(\mathbf{B}) \\ \mathbf{A}D_2(\mathbf{B}) \\ \vdots \\ \mathbf{A}D_L(\mathbf{B}) \end{bmatrix} \mathbf{S}^T \right\|_F \tag{19}$$

where $\tilde{\mathbf{Z}}_{..l}$, $l = 1, 2, \ldots, L$, are the noisy slices. We find the LS update for the polarization matrix $\mathbf{S}$ as

$$\hat{\mathbf{S}}^T = \begin{bmatrix} \hat{\mathrm{A}}D_1\left(\hat{\mathbf{B}}\right) \\ \hat{\mathrm{A}}D_2\left(\hat{\mathbf{B}}\right) \\ \vdots \\ \hat{\mathrm{A}}D_L\left(\hat{\mathbf{B}}\right) \end{bmatrix}^+ \begin{bmatrix} \tilde{\mathbf{Z}}_1 \\ \tilde{\mathbf{Z}}_2 \\ \vdots \\ \tilde{\mathbf{Z}}_L \end{bmatrix} \tag{20}$$

where $\hat{\mathbf{B}}$ and $\hat{\mathbf{A}}$ denote previously obtained estimates of $\mathbf{B}$ and $\mathbf{A}$.

According to Eq. (13), Eq. (18) and Eq. (20), the matrices $\mathbf{B}$, $\mathbf{A}$ and $\mathbf{S}$ are updated with conditioned least squares, respectively. The matrix update will stop until convergence. We can use TALS algorithm to attain the direction matrix $\mathbf{A}$ and the polarization matrix $\mathbf{S}$.

TALS algorithm is optimal when noise is additive i.i.d. Gaussian [43]. TALS yields maximum likelihood (ML) estimates for zero-mean white Gaussian noise [44]. TALS algorithm has several advantages: it is easy to implement, guarantee to converge and simple to extend to higher order data. The shortcomings are mainly in the occasional slowness of the convergence process [45]. In this paper, we use the COMFAC algorithm [46] for trilinear decomposition. COMFAC algorithm is essentially a fast implementation of TALS, and can speeds up the LS fitting. COMFAC algorithm is essentially a fast implementation of TALS, and can speeds up the LS fitting. COMFAC compresses the three-way data into a smaller three-way data. After fitting the model in the compressed space, the solution is decompressed to the original space. This is followed by a few TALS steps in uncompressed space. Usually, the decompressed model is close to the LS solution, hence smaller TALS steps are sufficient for this refinement stage. We can use COMFAC algorithm to attain the direction matrix $\mathbf{A}$ and the polarization matrix $\mathbf{S}$.

3.2. Identifiability

The k-rank concept is very important in the trilinear algebra.

Definition 1 [30]: Consider a matrix $\mathbf{U} \in \mathbb{C}^{I\times J}$. If $\text{rank}(\mathbf{U}) = r$, then $\mathbf{U}$ contains a collection of r linearly independent columns. Moreover, if every $l \leq J$ columns of $\mathbf{U}$ are linearly independent, but this does not hold for every $l+1$ columns, then $\mathbf{U}$ has k-rank$k_{\mathbf{U}} = l$. Note that $k_{\mathbf{U}} \leq \text{rank}(\mathbf{U}), \forall \mathbf{U}$.

Theorem 1 [30]: $\mathbf{X}_{..m} = \mathbf{S}D_m(\mathbf{A})\mathbf{B}^T$, $m = 1, 2, \ldots, M$, where $A \in \mathbb{C}^{M\times K}$, $\mathbf{S} \in \mathbb{C}^{3\times K}$, $\mathbf{B} \in \mathbb{R}^{L\times K}$, if

$$k_{\mathbf{A}} + k_{\mathbf{B}} + k_{\mathbf{S}} \geq 2K + 2 \tag{21}$$

Then $\mathbf{A}$, $\mathbf{B}$ and $\mathbf{S}$ are unique up to permutation and scaling of columns, that is to say any other matrices $\bar{\mathbf{A}}, \bar{\mathbf{B}}, \bar{\mathbf{S}}$ that constitute the $\mathbf{X}_{..m}$, $m = 1, 2, \ldots, M$ data is related to via

$$\bar{\mathbf{A}} = \mathbf{A}\Pi\Delta_1,\ \bar{\mathbf{B}} = \mathbf{B}\Pi\Delta_2,\ \bar{\mathbf{S}} = \mathbf{S}\Pi\Delta_3 \tag{22}$$

where Π is a permutation matrix, and $\Delta_1, \Delta_2, \Delta_3$ are diagonal scaling matrices satisfying scaling matrices satisfying

$$\Delta_1\Delta_2\Delta_3 = \mathbf{I} \tag{23}$$

Scale ambiguity and permutation ambiguity are inherent to the separation problem. This is not a major concern. Permutation ambiguity can be resolved by resorting to a priori or the embedded information. The scale ambiguity can be resolved using automatic gain control, normalization, differential encoding/decoding and the embedded information.

In our present context, for source-wise independent source signals, $k_{\mathbf{B}} = \min(K, L)$; for source-wise independent DOA, $k_{\mathbf{A}} = \min(M, K)$; for source-wise independent polarization, $k_{\mathbf{S}} = \min(3, K)$, and therefore, Eq. (21) becomes

$$\min(M, K) + \min(L, K) + \min(3, K) \geq 2K + 2 \tag{24}$$

For the received noisy signal, we use trilinear decomposition to get the estimated direction matrix and the polarization matrix $\hat{\mathbf{A}} = \mathbf{A}\Pi\Delta_1 + \mathbf{N}_1$, $\hat{\mathbf{S}} = \mathbf{S}\Pi\Delta_3 + \mathbf{N}_2$, where $\mathbf{N}_1$ and $\mathbf{N}_2$ are noise.

3.3. DOA Estimation

In general $\phi_0 = 0$, each element in $\mathbf{a}(\theta_q, \varphi_q)$ (direction vector for the qth source, as shown in Eq. (4)) is divided by the first element, and we

removes the first element to get an new vector $\mathbf{a}_1$, finally imag(ln($\mathbf{a}_1$)) is shown as follows, where ln(.) is natural logarithm; imag(.) is to get imaginary part of a complex number.

$$\begin{bmatrix} \xi \sin\theta_q \cos\varphi_q(\cos\phi_1 - 1) + \xi \sin\theta_q \sin\varphi_q \sin\phi_1 \\ \xi \sin\theta_q \cos\varphi_q(\cos\phi_2 - 1) + \xi \sin\theta_q \sin\varphi_q \sin\phi_2 \\ \vdots \\ \xi \sin\theta_q \cos\varphi_q(\cos\phi_{M-1} - 1) + \xi \sin\theta_q \sin\varphi_q \sin\phi_{M-1} \end{bmatrix} \tag{25}$$

where $\xi = 2\pi R/\lambda$. In Eq. (25), ith element is divided by $(\cos\phi_i - 1)$, $i = 1, 2 \ldots, M-1$, then we get

$$\mathbf{g} = \begin{bmatrix} c_0 + c_1 \sin\phi_1/(\cos\phi_1 - 1) \\ c_0 + c_1 \sin\phi_2/(\cos\phi_2 - 1) \\ \vdots \\ c_0 + c_1 \sin\phi_{M-1}/(\cos\phi_{M-1} - 1) \end{bmatrix} \tag{26}$$

where $c_0 = \xi \sin\theta_q \cos\varphi_q$, $c_1 = \xi \sin\theta_q \sin\varphi_q$. And we can use least squares principle to estimate DOA.

The estimated direction vector $\hat{\mathbf{a}}_q$ is attained through trilinear decomposition. The estimated direction vector $\hat{\mathbf{a}}_q$ is processed through normalization, which can resolve scale ambiguity, and is processed like mentioned above to get $\hat{\mathbf{g}}$. Least squares fitting is

$$\mathbf{P} \begin{bmatrix} c_0 \\ c_1 \end{bmatrix} = \boldsymbol{\beta}_2 \tag{27}$$

where

$$\mathbf{P} = \begin{bmatrix} 1 & \sin\phi_1/(\cos\phi_1 - 1) \\ 1 & \sin\phi_2/(\cos\phi_2 - 1) \\ \vdots & \vdots \\ 1 & \sin\phi_{M-1}/(\cos\phi_{M-1} - 1) \end{bmatrix} \tag{28}$$

We use least square principle to estimate $\begin{bmatrix} c_0 \\ c_1 \end{bmatrix}$

$$\begin{bmatrix} \hat{c}_0 \\ \hat{c}_1 \end{bmatrix} = \left(\mathbf{P}^T\mathbf{P}\right)^{-1} \mathbf{P}^T \boldsymbol{\beta}_2 \tag{29}$$

DOA estimation

$$\hat{\theta}_q = \sin^{-1}\left(\sqrt{\hat{c}_0^2 + \hat{c}_1^2}/\xi\right) \tag{30}$$

$$\hat{\varphi}_q = \tan^{-1}(\hat{c}_1/\hat{c}_0) \tag{31}$$

3.4. Polarization Estimation

Define $u = \sin\gamma_q e^{j\eta_q}$, $v = \cos\gamma_q$. According to the estimated angles $(\hat{\theta}_q, \hat{\varphi}_q)$ and Eq. (2), the estimated vector of $\begin{bmatrix} \sin\gamma_q e^{j\eta_q} \\ \cos\gamma_q \end{bmatrix}$ is

$$\begin{bmatrix} \hat{u} \\ \hat{v} \end{bmatrix} = \begin{bmatrix} \cos\hat{\theta}_q\cos\hat{\varphi}_q & -\sin\hat{\varphi}_q \\ \cos\hat{\theta}_q\sin\hat{\varphi}_q & \cos\hat{\varphi}_q \\ -\sin\hat{\theta}_q & 0 \end{bmatrix}^{+} \hat{\mathbf{s}}_q \tag{32}$$

where $[.]^+$ stands for pseudo-inverse. $\hat{\mathbf{s}}_q$ is the estimated polarization vector through trilinear decomposition. According to Eq. (32), polarization parameter γ_q is estimated by

$$\hat{\gamma}_q = \tan^{-1}\left(\left|\frac{\hat{u}}{\hat{v}}\right|\right) \tag{33}$$

According to Eq. (32) and Eq. (33), polarization parameter η_q is estimated by

$$\hat{\eta}_q = \text{imag}\left(\ln\left(\frac{\hat{u}}{\hat{v}\tan(\hat{\gamma}_q)}\right)\right) \tag{34}$$

where imag(.) is to get imaginary part of a complex number.

3.5. Blind DOA and Polarization Estimation Algorithm

Trilinear decomposition-based blind joint DOA and polarization estimation for polarization sensitive uniform circular array is proposed in this paper. This algorithm firstly uses COMFAC for trilinear decomposition to attain the direction matrix and polarization matrix, and then estimate DOA according to the estimated direction matrix, finally estimate polarization according to the estimated DOA and the estimated polarization matrix.

It should be pointed out that ESPRIT is a special case of trilinear model. ESPRIT is two-slice eigen analysis method, which is used to parameter estimation via two-slices. Trilinear decomposition method can be thought of as a generalization of ESPRIT.

4. SIMULATION RESULTS

According to Eq. (10), we define SNR

$$SNR = 10\log_{10}\frac{\sum_{m=1}^{M}\left\|\mathbf{S}D_m(\mathbf{A})\mathbf{B}^T\right\|^2}{\sum_{m=1}^{M}\left\|\mathbf{V}_{..m}\right\|^2}d\mathbf{B} \tag{35}$$

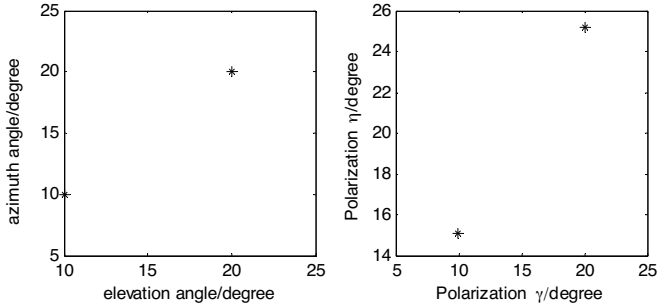

Figure 3. DOA and polarization estimation scatter with $K = 2$, $L = 100$ and $SNR = 28\,\mathrm{dB}$.

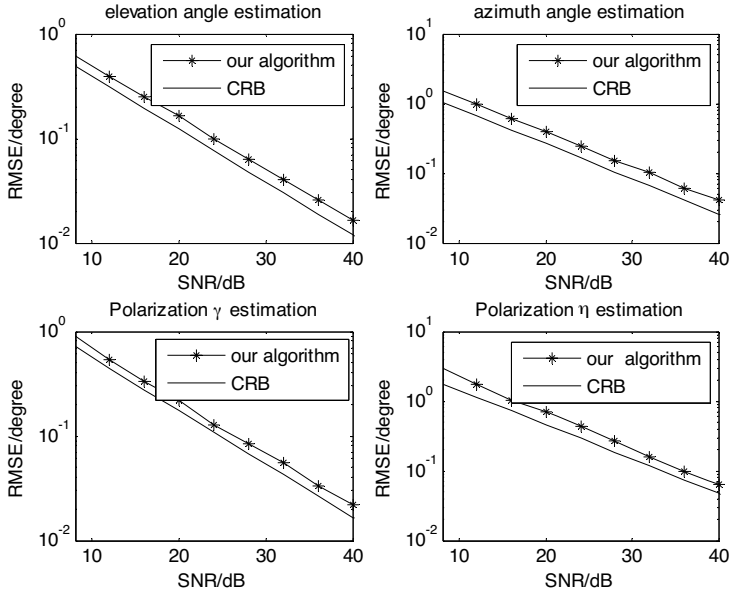

Figure 4. DOA and polarization estimation performance with $K = 2$ and $L = 100$.

We present Monte Carlo simulations to assess the DOA and polarization performance of our proposed algorithm. The number of Monte Carlo trials is 1000.

The uniform circular array with 8 diversely-polarized-antennas is used in the simulations. The antennas are considered to be completely polarized. Complex additive Gaussian white noise is added into this system. Define $RMSE = \sqrt{\frac{1}{1000}\sum_{m=1}^{1000}|a_m - a_0|^2}$, where a_m is the estimated DOA/polarization of the mth time; a_0 is the perfect DOA/polarization.

Note that K is the number of sources and L is the number of snapshots.

Simulation 1: There are 2 sources in this simulation. Their DOAs are (10°, 10°), (20°, 20°), and their corresponding polarization parameters (γ, η) are (10°, 15°), (20°, 25°). Fig. 3 shows the DOA and polarization scatters with $K = 2$, $L = 100$ and $SNR = 28$ dB. From Fig. 3, we find that our proposed algorithm works well. Fig. 4 presents the DOA and polarization estimation performance under different SNR. We also compared our proposed algorithm with Cramer-Rao bound CRB. From Fig. 4, we find that our proposed algorithm has better DOA and polarization estimation performance.

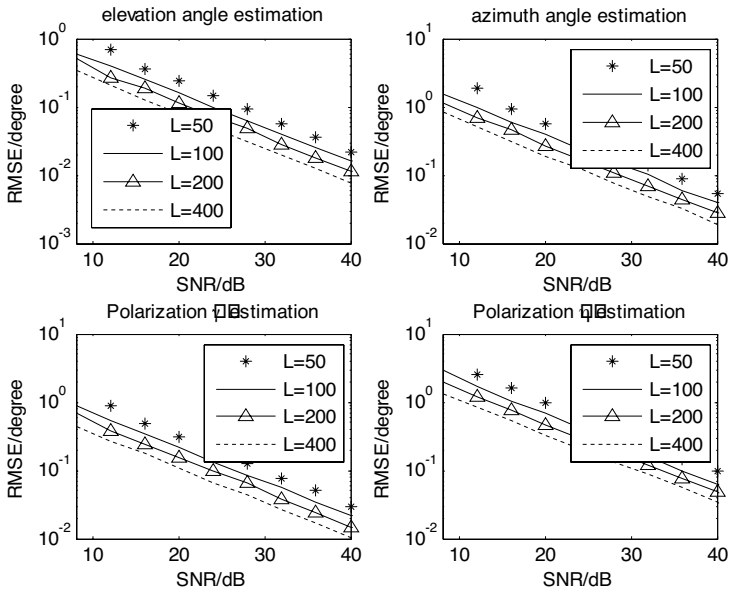

Figure 5. DOA and polarization estimation performance with different L.

Simulation 2: The performance of the algorithm under different L is shown in Fig. 5. There are 2 sources in this simulation. Their DOAs are (10°, 10°), (20°, 20°), and their corresponding polarization parameters (γ, η) are (10°, 15°), (20°, 25°). Fig. 5 shows the elevation angle, azimuth angle and polarization parameter (γ, η) estimation performance with different L. From Fig. 5, we find that when L becomes larger, the DOA and polarization estimation performance of our proposed algorithm gets better.

Simulation 3: The performance of our proposed algorithm under different source number K is investigated in the simulation. The source number is set 2, 3 and 4. The number of snapshots is 100. Our proposed algorithm has the different performance under different source number, as shown in Fig. 6. Fig. 6 presents the elevation angle, azimuth angle and polarization parameter (γ, η) estimation performance under different K. From Fig. 6, we find that DOA and polarization estimation performance of our proposed algorithm degrades with the increasing of the source number K.

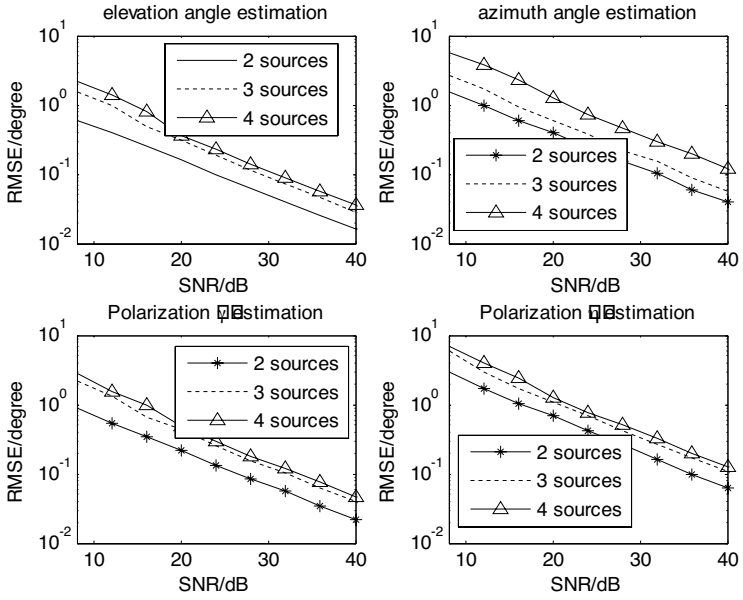

Figure 6. DOA and polarization estimation performance with different source.

5. CONCLUSION

This paper links the polarization-sensitive uniform circular array parameter estimation problem to the trilinear model and derives a novel blind DOA and polarization estimation. Our proposed algorithm has better DOA and polarization estimation performance. This algorithm does not require pilot information and train sequence. Instead, this method relies on a fundamental result of Kruskal regarding the uniqueness of low-rank three-way data decomposition. Compared with ESPRIT method, our proposed algorithm is the generalization of ESPRIT. ESPRIT method is a special case of our proposed algorithm. ESPRIT can work well in polarization-sensitive uniform linear array or uniform square array, but ESPRIT fails to work in polarization-sensitive uniform circular array. Our proposed algorithm has wider application than ESPRIT method, and our proposed algorithm can work well in polarization-sensitive uniform linear array, uniform circular array, L-shape array and uniform square array.

ACKNOWLEDGMENT

This work is supported by China NSF Grants (60801052) and Jiangsu NSF Grants (BK2007192). The authors wish to thank the anonymous reviewers for their valuable suggestions on improving this paper.

REFERENCES

1. Costanzo, S. and G. Dimassa, "Direct far-field computation from bi-polar near-field samples," *Journal of Electromagnetic Waves and Applications*, Vol. 20, No. 9, 1137–1148, 2006.
2. Bao, X. L. and M. J. Ammann, "Comparison of several novel annular-ring microstrip patch antennas for circular polarization," *Journal of Electromagnetic Waves and Applications*, Vol. 20, No. 11, 1427–1438, 2006.
3. Zheng, J.-P. and K. Kobayashi, "Plane wave diffraction by a finite parallel-plate waveguide with four-layer material loading: Part I - The case of E polarization," *Progress In Electromagnetics Research B*, Vol. 6, 1–36, 2008.
4. Shang, E.-H. and K. Kobayashi, "Plane wave diffraction by a finite parallel-plate waveguide with four-layer material loading: Part II - The case of H polarization," *Progress In Electromagnetics Research B*, Vol. 6, 267–294, 2008.

5. Chen, Y.-B., T.-B. Chen, Y.-C. Jiao, and F.-S. Zhang, "A reconfigurable microstrip antenna with switchable polarization," *Journal of Electromagnetic Waves and Applications*, Vol. 20, No. 10, 1391–1398, 2006.
6. Bao, X. L. and M. J. Ammann, "Comparison of several novel annular-ring microstrip patch antennas for circular polarization," *Journal of Electromagnetic Waves and Applications*, Vol. 20, No. 11, 1427–1438, 2006.
7. Liu, W. C. and P.-C. Kao, "Design of a probe-fed h-shaped microstrip antenna for circular polarization," *Journal of Electromagnetic Waves and Applications*, Vol. 21, No. 7, 857–864, 2007.
8. Zhang, M.-T., Y.-B. Chen, and Y.-C. Jiao, "Dual circularly polarized antenna of compact structure for radar application," *Journal of Electromagnetic Waves and Applications*, Vol. 20, No. 14, 1895–1902, 2006.
9. Panagopoulos, A. D. and G. E. Chatzaraki, "Outage performance of single/dual polarized fixed wireless access links in heavy rain climatic regions," *Journal of Electromagnetic Waves and Applications*, Vol. 21, No. 3, 283–297, 2007.
10. Ng, J. W. P. and A. Manikas, "Polarisation-sensitive array in blind MIMO CDMA system," *Electronics Letters*, Vol. 41, No. 17, 49–50, 2005.
11. Tu, T.-C., C.-M. Li, and C.-C. Chiu, "The performance of polarization diversity schemes in outdoor micro cells," *Progress In Electromagnetics Research*, PIER 55, 175–188, 2005.
12. Ioannis, K. and G. B. Keith, "Base station polarization-sensitive adaptive antenna for mobile radio," *Third Annual International Conference on Universal Personal Communications*, 230–235, 1994.
13. Lizzi, L., F. Viani, M. Benedetti, P. Rocca, and A. Massa, "The M-DSO-ESPRIT method for maximum likelihood DOA estimation," *Progress In Electromagnetics Research*, PIER 80, 477–497, 2008.
14. Gu, Y.-J., Z.-G. Shi, K. S. Chen, and Y. Li, "Robust adaptive beamforming for steering vector uncertainties based on equivalent DOAs method," *Progress In Electromagnetics Research*, PIER 79, 277–290, 2008.
15. Lie, J. P., B. P. Ng, and C. M. See, "Multiple UWB emitters DOA estimation employing time hopping spread spectrum," *Progress In Electromagnetics Research*, PIER 78, 83–101, 2008.

16. Mukhopadhyay, M., B. K. Sarkar, and A. Chakrabarty, "Augmentation of anti-jam GPS system using smart antenna with a simple DOA estimation algorithm," *Progress In Electromagnetics Research*, PIER 67, 231–249, 2007.
17. Harabi, F., H. Changuel, and A. Gharsallah, "Direction of arrival estimation method using a 2-L shape arrays antenna," *Progress In Electromagnetics Research*, PIER 69, 145–160, 2007.
18. Lundback, J. and S. Nordebo, "Analysis of a tripole array for polarization and direction of arrival estimation," *2004 IEEE Sensor Array and Multichannel Signal Processing Workshop Proceedings*, 284–288, July 2004.
19. Li, J. and R. T. Compton, "Angle and polarization estimation using ESPRIT with a polarization sensitive array," *IEEE Transactions on Antennas and Propagation*, Vol. 39, No. 9, 1376–1383, 1991.
20. Wong, K. T. and M. D. Zoltowski, "Uni-vector-sensor ESPRIT for multi-source azimuth-elevation angle estimation," *IEEE Transactions on Antennas and Propagation*, Vol. 45, No. 10, 1467–1474, 1997.
21. Li, J. and R. T. Compton, "Two-dimensional angle and polarization estimation using the ESPRIT algorithm," *IEEE Transactions on Antennas and Propagation*, Vol. 40, No. 5, 550–555, 1992.
22. Chen, F.-J., S. Kwong, and C.-W. Kok, "Two-dimensional angle and polarization estimation using ESPRIT without pairing," *2006 IEEE International Symposium on Circuits and Systems*, 1063–1066, May 2006.
23. Yuan, Q., Q. Chen, and K. Sawaya, "MUSIC based DOA finding and polarization estimation using USV with polarization sensitive array antenna," *2006 IEEE Radio and Wireless Symposium*, 339–342, Jan. 17–19, 2006.
24. Wong, K. T., L. S. Li, and M. D. Zoltowski, "Root-MUSIC-based direction finding and polarization estimation using diversely polarized possibly collocated antennas," *IEEE Antennas and Wireless Propagation Letters*, No. 3, 129–132, 2004.
25. Egemen, G. and J. M. Mendel, "Applications of cumulants to array processing — Part VI: Polarization and direction of arrival estimation with minimally constrained arrays," *IEEE Transactions on Antennas and Propagation*, Vol. 47, No. 9, 2589–2591, 1999.
26. Zhang, Q., L. Wang, Y. Wang, et al., "Cyclostationarity-based DOA and polarization estimation for multipath signals with a

uniform linear array of electromagnetic vector sensors," *2006 International Conference on Machine Learning and Cybernetics*, 2047–2052, Aug. 2006.

27. Richter, A., F. Belloni, and V. Koivunen, "DoA and polarization estimation using arbitrary polarimetric array configurations," *IEEE Workshop Sensor Array and Multichannel Signal Processing*, 55–59, July 2006.
28. Wong, K. T. and M. D. Zoltowski, "Closed-form direction finding and polarization estimation with arbitrarily spaced electromagnetic vectorsensors at unknown locations," *IEEE Transactions on Antennas and Propagation*, Vol. 48, No. 5, 671–681, 2000.
29. Zainud-Deen, S. H., H. Malhat, K. H. Awadalla, and E. S. El-Hadad, "Direction of arrival and state of polarization estimation using radial basis function neural network (RBFNN)," *Progress In Electromagnetics Research B*, Vol. 2, 137–150, 2008.
30. Kruskal, J. B., "Three-way arrays: Rank and uniqueness of trilinear decompositions, with application to arithmetic complexity and statistics," *Linear Algebra Applicat.*, Vol. 18, 95–138, 1977.
31. Pham, T. D. and J. Mocks, "Beyond principal component analysis: A trilinear decomposition model and least squares estimation," *Psychometrika*, Vol. 57, No. 2, 203–215, 1992.
32. Wu, H.-L., R.-Q. Yu, and K. Oguma, "Trilinear component analysis in modern analytical chemistry," *Anal. Sci.*, Vol. 17, No. 4, 1483–1486, 2001.
33. Wise, B. M., N. B. Gallagher, S. W. Butler, D. D. White, and G. G. Barna, "A comparison of principal component analysis, multiway principal component analysis, trilinear decomposition and parallel factor analysis for fault detection in a semiconductor etch process," *Journal of Chemometrics*, Vol. 13, 379–396, 1999.
34. Henrion, R. and C. A. Andersson, "A new criterion for simple-structure core transformations in N-way principal components analysis," *Chemom. Intell. Lab. Syst.*, Vol. 47, 189–204, 1999.
35. De Lathauwer, L., B. De Moor, and J. Vandewalle, "Computation of the canonical decomposition by means of a simultaneous generalized schur decompositition," *SIAM J. Matrix Anal. Appl.*, Vol. 26, No. 2, 295–327, 2004.
36. De Lathauwer, L., "A link between the canonical decomposition in multilinear algebra and simultaneous matrix diagonalization," *SIAM J. Matrix Anal. Appl.*, Vol. 28, No. 3, 642–666, 2006.

37. Zhang, X. and D. Xu, "PARAFAC multiuser detection for SIMO-CDMA system," *2006 International Conference on Communications, Circuits and Systems Proceedings*, 744–747, 2006.
38. Zhang, X. and D. Xu, "Parallel factor analysis based blind space-time multiuser detection for CDMA system with larger delay spread channel," *Journal of Nanjing University of Aeronautics & Astronautics*, Vol. 39, No. 2, 204–207, 2007.
39. Yue, R., S. A. Vorobyov, A. B. Gershman, and N. D. Sidiropoulos, "Blind spatial signature estimation via time-varying user power loading and parallel factor analysis," *IEEE Transactions on Signal Processing*, Vol. 53, No. 5, 1697–1710, 2005.
40. Sidiropoulos, N. D. and X. Liu, "Identifiability results for blind beamforming in incoherent multipath with small delay spread," *IEEE Transactions on Signal Processing*, Vol. 49, No. 1, 228–236, 2001.
41. Yu, Y. and A. P. Petropulu, "Parafac based blind estimation of MIMO systems with possibly more inputs than outputs," *2006 IEEE International Conference on Acoustics, Speech and Signal Processing,* Vol. 3, 133–136, May 2006.
42. Mokios, K. N., N. D. Sidiropoulos, and A. Potamianos, "Blind speech separation using parafac analysis and integer least squares," *2006 IEEE International Conference on Acoustics, Speech and Signal Processing*, 73–76, May 2006.
43. Vorobyov, S. A., Y. Rong, N. D. Sidiropoulos, et al., "Robust iterative fitting of multilinear models," *IEEE Transactions on Signal Processing*, Vol. 53, No. 8, 2678–2689, 2005.
44. Liu, X. and N. Sidiropoulos, "Cramer-Rao lower bounds for low-rank decomposition of multidimensional arrays," *IEEE Transactions on Signal Processing*, Vol. 49, No. 9, 2074–2086, 2001.
45. Tomasi, G. and R. Bro, "A comparison of algorithms for fitting the PARAFAC model," *Computational Statistics & Data Analysis*, Vol. 50, 1700–1734, 2006.
46. Bro, R., N. D. Sidiropoulos, and G. B. Giannakis, "A fast least squares algorithm for separating trilinear mixtures," *Int. Workshop Independent Component and Blind Signal Separation Anal.*, Aussois, France, Jan. 11–15, 1999.